Constraint on a variation of the proton-to-electron mass ratio from H2 absorption towards quasar Q2348-011

Bagdonaite, J.; Murphy, M.T.; Kaper, L.; Ubachs, W.

DOI
10.1111/j.1365-2966.2011.20319.x

Publication date
2012

Document Version
Final published version

Published in
Monthly Notices of the Royal Astronomical Society

Monthly Notices
of the
ROYAL ASTRONOMICAL SOCIETY

Mon. Not. R. Astron. Soc. **421,** 419–425 (2012) doi:10.1111/j.1365-2966.2011.20319.x

Constraint on a variation of the proton-to-electron mass ratio from H_2 absorption towards quasar Q2348−011

Julija Bagdonaite,[1⋆] Michael T. Murphy,[2⋆] Lex Kaper[1,3⋆] and Wim Ubachs[1⋆]

[1]*Department of Physics and Astronomy, LaserLaB, VU University, De Boelelaan 1081, 1081 HV Amsterdam, the Netherlands*
[2]*Centre for Astrophysics and Supercomputing, Swinburne University of Technology, Victoria 3122, Australia*
[3]*Astronomical Institute Anton Pannekoek, Universiteit van Amsterdam, 1098 SJ Amsterdam, the Netherlands*

Accepted 2011 December 1. Received 2011 December 1; in original form 2011 November 18

ABSTRACT

Molecular hydrogen (H_2) absorption features observed in the line of sight to Q2348−011 at redshift $z_{\rm abs} \simeq 2.426$ are analysed for the purpose of detecting a possible variation of the proton-to-electron mass ratio $\mu \equiv m_{\rm p}/m_{\rm e}$. By its structure, Q2348−011 is the most complex analysed H_2 absorption system at high redshift so far, featuring at least seven distinctly visible molecular velocity components. The multiple velocity components associated with each transition of H_2 were modelled simultaneously by means of a comprehensive fitting method. The fiducial model resulted in $\Delta\mu/\mu = (-0.68 \pm 2.78) \times 10^{-5}$, showing no sign that μ in this particular absorber is different from its current laboratory value. Although not as tight a constraint as other absorbers have recently provided, this result is consistent with the results from all previously analysed H_2-bearing sightlines. Combining all such measurements yields a constraint of $|\Delta\mu/\mu| \leq 10^{-5}$ for the redshift range $z = 2$–3.

Key words: methods: data analysis – quasars: absorption lines – cosmology: observations.

1 INTRODUCTION

The spectrum of molecular hydrogen is known to be a testing ground to search for temporal variation of the proton-to-electron mass ratio, $\mu \equiv m_{\rm p}/m_{\rm e}$, on cosmological time-scales (Thompson 1975). The spectral lines of the Lyman and Werner absorption bands of H_2 shift into an atmospheric transmission window ($\lambda > 3050$ Å) for absorption systems at redshift $z \gtrsim 2$, and thus become observable with ground-based optical telescopes. Wavelengths of H_2 spectral lines as observed in high-redshift absorption systems are compared to the wavelengths measured in the laboratory for which now very accurate calibrations exist (Philip et al. 2004; Salumbides et al. 2008; Bailly et al. 2010) as well as for the HD isotopologue (Ivanov et al. 2008; Ivanov et al. 2010), which is currently also detected at high redshift. Values for the sensitivity coefficients, K_i, expressing the shift of each spectral line as a result of a drifting μ, have been established to sufficient accuracy for H_2 (Meshkov et al. 2006; Ubachs et al. 2007). Hence a condition is accomplished that searches for cosmological μ variation via H_2 spectra solely depend on the accuracy of the astrophysical data.

From the large number of damped Lyman α systems (DLAs) identified only some 20 are known to harbour detectable H_2 spectral features (Ledoux, Petitjean & Srianand 2003; Srianand et al. 2005; Ubachs et al. 2007). As was discussed recently (Ubachs et al. 2011) only a handful of those high-redshift absorption systems can deliver an H_2 spectrum of sufficient quality, i.e. a reasonable signal-to-noise ratio (S/N) on the continuum level to be obtained in reasonable data collection times at large-dish telescopes, and a large number of H_2 transitions ($\gtrsim$50). The high-quality spectra of the Q0347−383 and Q0405−443 systems obtained with the European Southern Observatory (ESO) Very Large Telescope (VLT) equipped with the high-resolution Ultraviolet and Visible Echelle Spectrograph (UVES) initially yielded an indication for a possible drift in μ, which is expressed via $\Delta\mu/\mu \equiv (\mu_z - \mu_{\rm lab})/\mu_{\rm lab}$ (Reinhold et al. 2006). A more sophisticated re-analysis of the same spectra by the so-called comprehensive fitting method, also invoking an improved thorium–argon (Th–Ar) calibration, reduced the initial finding of a 4σ effect of a positive $\Delta\mu/\mu$ to a 1.5–2.0σ effect (King et al. 2008). The same spectra were also re-analysed by Wendt & Reimers (2008) and by Thompson et al. (2009), while Wendt & Molaro (2010) re-observed Q0347−383 with VLT-UVES to find a 1.5σ effect. The highest quality system observed so far is J2123−0050. Observations with both the Keck Telescope (Malec et al. 2010) and VLT (van Weerdenburg et al. 2011) were incorporated in a μ-variation analysis. The two studies yielded constraints on $\Delta\mu/\mu$ which are in very good agreement with each other. The averaged constraint for J2123−0050 is $\Delta\mu/\mu = (7.6 \pm 3.5) \times 10^{-6}$. The system Q0528−250 has been at the heart of μ-variation analyses since the first attempts by Varshalovich & Levshakov (1993) to derive a constraint on $\Delta\mu/\mu$ from a low-resolution spectrum. King et al. (2008) derived a tight constraint from a comprehensive fitting analysis of a VLT spectrum of Q0528−250; a recent re-observation

⋆E-mail: j.bagdonaite@vu.nl (JB); mmurphy@swin.edu.au (MTM); L.Kaper@uva.nl (LK); w.m.g.ubachs@vu.nl (WU)

of this high-quality system, again at VLT, confirmed the previous conclusion of a tight constraint on $\Delta\mu/\mu$ (King et al. 2011). Based on the combined results derived from high-redshift H_2 absorbers it can be concluded that $|\Delta\mu/\mu| < 1 \times 10^{-5}$ for redshifts $z = 2$–3.

The present study presents a detailed analysis of the search for μ-variation of an absorber system towards the quasar Q2348−011. The physical conditions of this system had been investigated before based on data from the VLT (Ledoux et al. 2006; Petitjean et al. 2006; Noterdaeme et al. 2007). Q2348−011 was shown to be an exceptional sightline, with a number of DLAs and sub-DLAs present, and a very complex velocity structure in the major H_2 absorbing system at $z \simeq 2.426$. At least seven distinctly visible absorption features are associated with each H_2 transition in this system, while in other quasar sightlines H_2 absorption (if detected) exhibits much simpler profiles consisting typically of one or two features. For the present study, dedicated observations were performed at VLT focusing on improvement of S/N and on wavelength calibration of the spectrum. A preliminary μ-variation analysis of this absorber was presented in Ubachs et al. (2011). The current work improves upon the analysis but the constraint on Δ/μ is of similar precision as presented previously. It is demonstrated that a complex velocity structure consisting of at least seven distinct H_2 velocity features can be disentangled by the method of comprehensive fitting (King et al. 2008, 2011; Malec et al. 2010).

2 DATA

The new spectrum of the quasar Q2348−011 was obtained with the UVES spectrograph on the ESO VLT on four consecutive nights (2008 August 18–21). Q2348−011 is not a particularly bright object ($R = 18.31$) so a long exposure time was required. 15 exposures were taken, making up a combined total of 19.25 h of observation. After each science exposure, without any intervening grating resets, a Th–Ar exposure was recorded for calibration purposes. Seeing was in the range between 0.53 and 2.32 arcsec. Besides the exposures noted above, the final spectrum incorporates data obtained from the ESO data archive (observations from 2003 October 29 to 30). They contribute additional 4.50 h but do not have the individually taken Th–Ar calibration frames.

The raw 2D exposures were bias-corrected, flat-fielded, and the quasar flux extracted using the Common Pipeline Language version of the UVES pipeline.[1] The wavelength calibration was established by extracting each Th–Ar frame using the object profile weights from its corresponding quasar exposure. Further details of the wavelength calibration procedure are described in Murphy et al. (2007). The rms wavelength calibration residuals were typically $\approx$70 m s^{-1} in the Lyman α forest portion of the spectrum, where the H_2 lines fall. The wavelength scale of each quasar exposure was corrected from air to vacuum, and to the heliocentric reference frame, and the flux was re-dispersed on to a common log-linear scale before being co-added, using UVES_POPLER,[2] a code specifically written to re-disperse and combine reduced exposures from UVES.

The spectrum of Q2348−011 covers wavelengths 3572–9467 Å, with gaps at 4520–4621 and 7505–7665 Å. The final spectrum has a resolving power of $R \sim 57\,000$ and 63 000, and the log-linear dispersion is set to 2.5 and 1.5 km s^{-1} in the blue (<4000 Å) and in the red (>4000 Å) parts, respectively. CCD pixels were binned by a factor of 2 in both spatial and spectral directions for all exposures in the blue, and no binning was applied for the red exposures. In the blue part where H_2 features are detected the average S/N ratio is about 25.

3 THE COMPREHENSIVE FITTING METHOD

The main aim of the present analysis is to determine the spectral positions of the H_2 absorption features present in a quasar spectrum as accurately as possible since their overall pattern defines the value of $\Delta\mu/\mu$: each absorption line of the H_2 Lyman and Werner bands shows a unique shift for a given change of μ that depends on the vibrational and rotational quantum numbers of the upper and lower energy states. The shifted wavelength λ_i is related to the rest wavelength λ_0 by

$$\lambda_i = \lambda_0(1+z)\left(1 + K_i\frac{\Delta\mu}{\mu}\right), \quad (1)$$

where z is the redshift of the absorber, and K_i is the sensitivity coefficient, different for each line. To achieve this goal a so-called comprehensive fitting method can be applied. This method requires fitting the absorption profiles of multiple H_2 transitions simultaneously. It relies on a physical assumption that all transitions arise from the same cloud (collection of clouds) of molecular hydrogen and, therefore, they share the parameters describing the properties of the clouds (see e.g. Malec et al. 2010).

Each H_2 transition can be detected in one or several absorption features depending on how many molecular hydrogen clouds are penetrated by the light of the quasar. We refer to each fitted component as a velocity component, as they are situated closely in velocity space. It is assumed that a given velocity component has the same redshift, $z_{\rm abs}$, and Doppler width, b, in all transitions independent of the rotational level, J. Each J level has a different population, represented by the column density N, but for a given velocity component it is the same for all transitions from the same J level. To analyse the spectrum we use the Voigt profile fitting program VPFIT,[3] which permits to tie the free parameters between various transitions. The optimal model is found by fitting all suitable transitions at the same time.

The differential shifts of the molecular hydrogen lines are only known to be possible through the $\Delta\mu/\mu$ parameter (see equation 1). It is added as a free parameter after all other parameters have been optimized. The comprehensive fitting approach allows minimization of the number of free parameters in the fit and, thus, the reliability of the absorption model which eventually translates to the robustness of $\Delta\mu/\mu$ resulting from the model.

4 ANALYSIS

4.1 The absorption system

The wavelengths covered by the VLT-UVES spectrum provide 58 H_2 transitions for rotational levels $J = 0$–5. All the observed lines arise from the Lyman band. In Fig. 1 a couple of H_2 transitions are displayed. No lines of HD were detected in this system. In the ideal case, this spectrum would provide a sample of 58 × 7 molecular hydrogen absorption lines. However, not all of them are suitable for the analysis. First of all, the broad Lyman β of an additional DLA at

[1] http://www.eso.org/observing/dfo/quality/UVES/pipeline/pipe_reduc.html

[2] Developed and maintained by M. Murphy; see http://astronomy.swin.edu.au/~mmurphy/UVES_popler.

[3] http://www.ast.cam.ac.uk/~rfc/vpfit.html

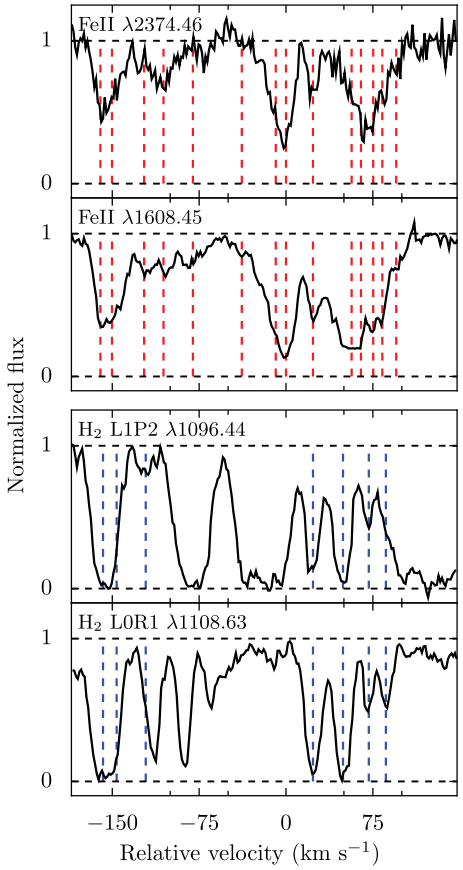

Figure 1. Two H_2 and two Fe II transitions are displayed on a common velocity scale, centred at $z_0 = 2.426\,3230$. In the H_2 velocity profile seven distinct features are visible, while the Fe II profiles consist of at least 14. Note that the third velocity component from the left in the H_2 L0R1 profile and the rightmost component in the H_2 L1P2 profile are blended with other intervening transitions in Lyman α forest. Due to such blends, the signal of at least seven absorption components is evident only when multiple H_2 transitions are explored simultaneously.

Table 1. A list of all the confirmed detections of metal absorbers in the spectrum of Q2348−011. Species whose transitions overlap some of the fitted H_2 regions are in bold.

Redshift	Species
0.774	Mg II
0.863	Mg II, Ca II
1.444	**C IV**, Mg II
2.426	C IV, Si IV, N V, C I, C I*, P II, Zn II, Al III, **Fe II**, S II, **Si II**
2.582	C IV, Si IV, Si II
2.615	C IV, Si IV, Fe II, Ni II, Cr II, Al II, **Si II**, **O I**, N I
2.739	C IV, **O I**
2.929	C IV, **Si IV**
2.969	C IV, N V

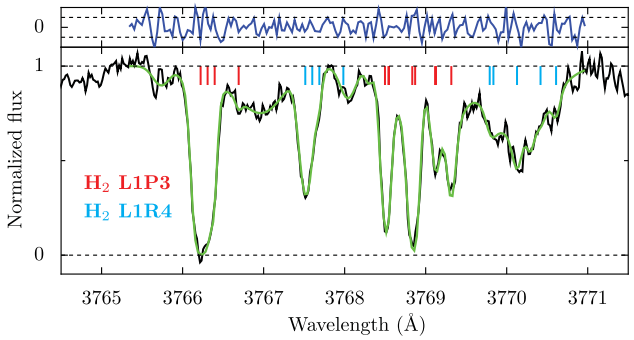

Figure 2. H_2 absorption profiles of two transitions L1P3 and L1R4, resulting from the fiducial model. Since the absorption arises in multiple widely spread components (indicated by the red tick marks for L1P3, and by the blue tick marks for L1R4), the two profiles overlap. The upper graph shows the normalized residuals of the fit; the dashed lines mark $\pm 1\sigma$ limits.

$z \simeq 2.62$ falls in the wavelength range where H_2 lines are detected, namely near 3710 Å. The break at $\lesssim$3590 Å might be produced by another absorber at $z \simeq 2.93$. These features make some of the H_2 transitions unavailable, and strongly damp some others. Also, the weaker H I absorbers of the Lyman α forest contaminate many of the regions with H_2 lines. Generally, the sightline of the Q2348−011 is rich in absorbing systems. The full list of detected metal absorbers is given in Table 1. Some of the absorbers have their metal absorption lines overlapped with H_2 lines. The metal absorption profiles are constrained by fitting their counterparts in the red part, e.g. Fe II λ1096 of the $z \simeq 2.426$ absorber can be constrained by tying it with Fe II λ1608.

Since the velocity structure of H_2 consists of at least seven velocity features spread over $\sim 250\,\mathrm{km\,s^{-1}}$, nearby lying transitions exhibit mutual overlap of velocity components. The self-blending of the H_2 transitions was often the decisive factor when setting the boundaries of usable fitting regions (i.e. regions over which χ^2 was calculated): only rarely did they include just one transition (see Fig. 2, as an example).

23 regions with 32 different molecular hydrogen transitions and eight regions with relevant metal absorption profiles were selected for further analysis. Although the total number of H_2 transitions available in this spectrum is reduced due to blends with H I lines, the scarcity of information is at least partially compensated for by the presence of multiple velocity components associated with each transition. Altogether, each transition contributes a higher information content when it is imprinted on several velocity components. A part of the spectrum with all available and all fitted H_2 transitions indicated is provided in Fig. 3.

4.2 Exploring the velocity structure of H_2

Seven absorption features can be distinguished by eye in the velocity structure of molecular hydrogen in the Q2348−011 spectrum (see Fig. 1, also Noterdaeme et al. 2007). However, as it was shown by Murphy, Webb & Flambaum (2008), a single spectral feature might need to be modelled by more than one velocity component, so it is plausible that in the case of Q2348−011 more than seven velocity components are actually required to produce a model which is both physically realistic and statistically acceptable. If a single Voigt profile is fitted to a feature which seems single but another weaker blending line is actually present, then the centroid returned from this fit will be shifted towards the blending line. The centroid wavelength of the fitted feature might be expressed as the intensity-weighted mean of the two blended lines. The positions of the lines play a crucial role in μ-variation analysis and this kind of underfitting may affect the results and therefore should be avoided.

The approach to reaching the optimal model of H_2 absorption is to keep adding velocity components until a statistically acceptable

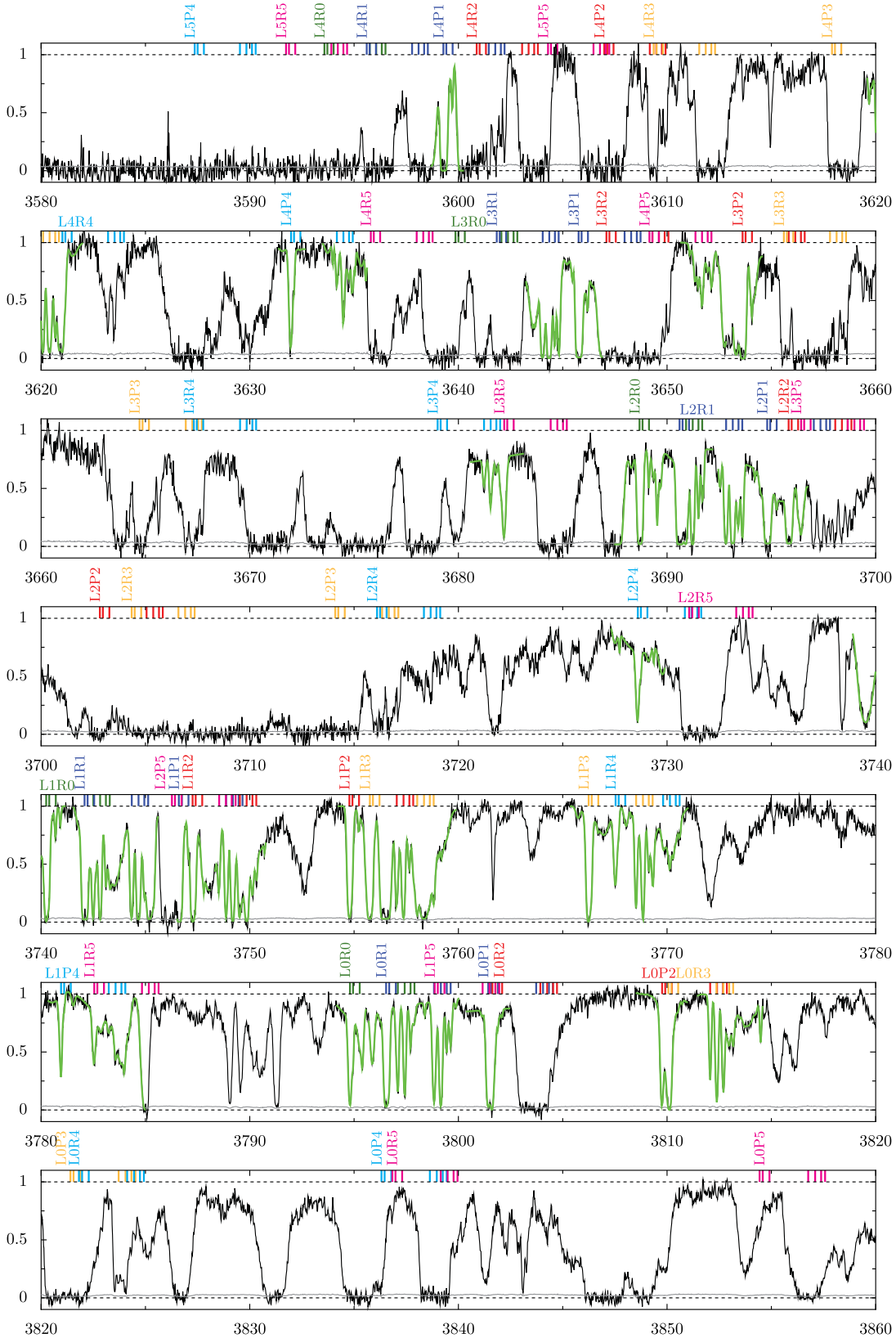

Figure 3. The part of the Q2348−011 spectrum containing the H_2 transitions. Transitions from different J levels are labelled in different colours. The associated ticks show positions of the seven (visually distinguishable) velocity components. The broad absorption feature at 3710 Å is the Lyman β line of the H I absorber at $z \simeq 2.62$. The break at the shortest wavelengths is due to another H I absorber at $z \simeq 2.93$. The green line shows the fitted regions.

fit is achieved (e.g. Malec et al. 2010; King et al. 2011). The initial absorption model included seven velocity components of H_2. Voigt profile parameters (z, b, N) of corresponding components are tied as described in Section 3. Each of the included regions was revisited and refined many times until an adequate fit was reached. By adequate we mean that the normalized residuals in each of the fitted regions are not too large or too small (i.e. they are distributed around $[-1\sigma{:}1\sigma]$), and no long range correlations are seen in them. Finally, after the fit was optimized, a value for $\Delta\mu/\mu$ was determined.

In a subsequent step an additional component was added to the left side of the absorption profile (at $\approx -150\,\mathrm{km\,s^{-1}}$; see Fig. 1). The reduced chi-square, χ^2_ν, of this model is slightly better than that of the initial one with seven velocity components. The procedure of adding more components was continued further until they started to be rejected from most J levels (>12 component models). We note that several components get rejected from $J = 4$ and 5 transitions in all models. Generally, it is not unusual that weak components are omitted from the lowly populated J levels. The higher J levels are less populated than the lower J levels, so weak components of $J = 4$ and 5 transitions may not be detected. In addition, the Q2348−011 spectrum provides only a few useful regions with $J =$ 4 and 5 transitions, which is not enough to amplify the signal of the weak components.

It should be emphasized that $\Delta\mu/\mu$ is always introduced as a single additional parameter after all the other free parameters of the given model have been optimized. This ensures that $\Delta\mu/\mu$ is not biased away from zero in the process of determining which velocity structure is statistically preferred. On the other hand, it could mean that $\Delta\mu/\mu$ might be slightly biased *towards* zero because the preferred velocity structure might have 'fitted away' some of the relative shifts between transitions which a non-zero $\Delta\mu/\mu$ would have caused. However, given that many H_2 transitions are fitted simultaneously, the bias towards zero will be very weak.

Results of the various fitting runs are displayed in Fig. 4, together with the goodness-of-fit measure, χ^2_ν. As it can be seen in Fig. 4, the χ^2_ν monotonically decreases when more components are added.

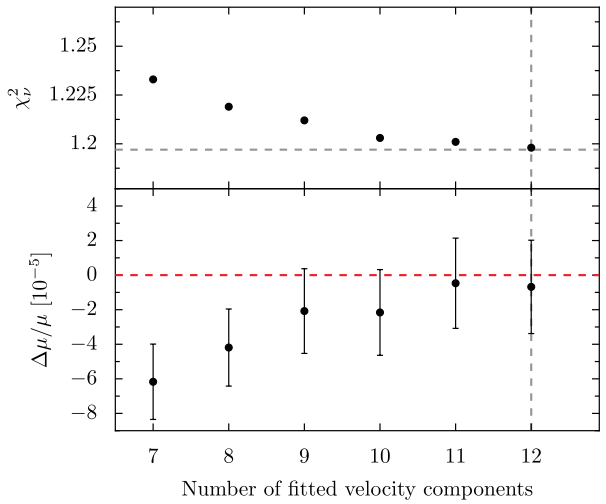

Figure 4. Lower graph: $\Delta\mu/\mu$ values as determined from various models. Error bars indicate estimated 1σ statistical uncertainties. Upper graph: χ^2_ν of the fit decreases as more components are added. A model with 12 components has the lowest χ^2_ν. Adding more components caused inconsistencies in the fit.

For models with 10, 11 and 12 components the difference in χ^2_ν is very small though. This is also true for the derived $\Delta\mu/\mu$ values – they match well within 1σ. For further analysis, the model with 12 velocity components has been adopted as fiducial.

4.3 Robustness of the model

When all available transitions are included in the 12-component model, the fit delivers $\Delta\mu/\mu = (-0.68 \pm 2.70_{\mathrm{stat}}) \times 10^{-5}$. Next the fiducial model is tested for its robustness. In the process of creating the model, many assumptions and decisions have been made, e.g. how parameters are tied between transitions and which regions are fitted. It can be tested how sensitive the value of $\Delta\mu/\mu$ determined from the model is to certain choices made. A description of several performed tests is given below, while the outcome is summarized in Table 2.

(i) The extended structure of the H_2 absorption profile can be divided into two parts. As it can be seen from velocity plots, the dividing line naturally falls at around $0\,\mathrm{km\,s^{-1}}$ (Fig. 1). When only the left part of the profile, which includes four H_2 velocity components, was used in the fitting, it resulted in $\Delta\mu/\mu = (3.55 \pm 4.34_{\mathrm{stat}}) \times 10^{-5}$. The right part with eight velocity components delivered $\Delta\mu/\mu = (-3.87 \pm 3.43_{\mathrm{stat}}) \times 10^{-5}$. The larger uncertainty of the left-side result can be explained by the fact that several of the fitted transitions were saturated, thus their centroids are determined less accurately. Altogether, the two results are consistent within the combined 1.3σ.

(ii) Instead of allowing all transitions to contribute to a single $\Delta\mu/\mu$ value, within VPFIT it is possible to fit a different value of $\Delta\mu/\mu$ for each J level or for J levels grouped in some way. This kind of test allows us to quantify the relative contributions different J levels make to the final result. As not many transitions are available in the Q2348−011 absorber, they were not investigated level by level. Ubachs et al. (2007) have suggested that H_2 transitions can be divided into a $J \in [0, 1]$ set (cold states) and a $J \geq 2$ set (warm states) to examine the impact of temperature: due to the para–ortho distribution of H_2 the $J = 1$ state is significantly populated even at low temperatures. A test was performed where only transitions from the cold states or only those from the warm states were used to determine $\Delta\mu/\mu$. The two values of $\Delta\mu/\mu$ match within the uncertainty. It means that the two groups of transitions contribute similarly to the final combined value of $\Delta\mu/\mu$.

(iii) All previously described tests were performed on absorption models which are based on the assumption that corresponding velocity components in all transitions have the same b-parameter, independent of rotational quantum state ($b \neq F[J]$). This assumption is relaxed to test what its effect is on $\Delta\mu/\mu$, i.e. in this run different J transitions are allowed to have different b-parameters in corresponding velocity components ($b = F[J]$). No significant discrepancy is found between the values determined from the $b \neq F[J]$ and the $b = F[J]$ models.

(iv) The spectrum used in the analysis includes exposures from the older 2003 ESO archive data set which do not have the individually taken Th–Ar calibration frames. They make up 4.50 h compared to 19.25 h of more accurately calibrated data. In order to make sure that the final result is not affected by the additional (possibly less accurate) data, they were excluded in one of the fit optimizations. The newly determined value is $\Delta\mu/\mu = (0.68 \pm 3.45_{\mathrm{stat}}) \times 10^{-5}$. The result is consistent with the one from the primary fit. The uncertainty is higher since the S/N of the spectrum used in this test is lower.

Table 2. Resulting $\Delta\mu/\mu$ values and their statistical uncertainties from various consistency tests performed on the 12 velocity component absorption model as described in Section 4.3. The $b \neq F[J]$ and the $b = F[J]$ models are different in that the former has b parameters tied in all J levels of corresponding velocity components whilst in the latter they are only tied within every J level of corresponding velocity components. The last line of the table refers to a test, in which only the best exposures (calibration wise) were included in the spectrum.

	b	Transitions	$n_{\rm trans}$	Components	$\Delta\mu/\mu$ ($\times 10^{-5}$)
	$\neq F[J]$	All	32	All	-0.68 ± 2.70
(i)	$\neq F[J]$	All	28	Left	3.55 ± 4.34
(i)	$\neq F[J]$	All	22	Right	-3.87 ± 3.43
(ii)	$\neq F[J]$	$J = [0, 1]$	11	All	-0.86 ± 3.50
(ii)	$\neq F[J]$	$J = [2–5]$	21	All	-0.46 ± 4.06
(iii)	$=F[J]$	All	32	All	-1.20 ± 3.03
(iv)	$\neq F[J]$	All	32	All	0.68 ± 3.45

The performed tests show that the final result on $\Delta\mu/\mu$ determined from the 12-component model is not affected by a subclass of transitions, velocity components or data.

4.4 Systematic errors

The statistical error of the fiducial result is larger than obtained in other recent studies of H_2 studies (e.g. Malec et al. 2010; King et al. 2011). In those studies, systematic errors were found to be smaller than, but comparable in magnitude to, the statistical errors. Thus, while it is still important to consider systematic errors in the present study, they are not expected to dominate the error budget.

Every echelle order included in the new Q2348−011 spectrum is calibrated using about 10 Th–Ar lines. The effect of the errors of individual Th–Ar lines is small (about 70 m s^{-1}) and random, so it will average out when many H_2 transitions spread over many orders are used. Murphy et al. (2007) have shown that possible systematic patterns in the Th–Ar calibration residuals result in a deviation of 30 m s^{-1} at most. The K_i values used in the present analysis are in the range from −0.015 to 0.018. The effect of the systematic errors can be expressed via: $\delta(\Delta\mu/\mu) = (\Delta v/c)/\Delta K_i$. A shift of 30 m s^{-1} translates to $\delta(\Delta\mu/\mu) = 0.3 \times 10^{-5}$, which is about 15 per cent of the statistical uncertainty.

In a recent study targeted at the possible miscalibration of the wavelength scale of the UVES spectrograph, it is reported that intra-order distortions of about 200 m s^{-1} in size may be present (Whitmore, Murphy & Griest 2010). Their influence can be roughly estimated by dividing the distortion by the square root of the number of the H_2 transitions included in the fit: $200/\sqrt{32} \approx 35$ m s^{-1}.

Malec et al. (2010) have considered additional sources of possible systematic errors, but they are all of the same order as the Th–Ar wavelength calibration uncertainties and are not expected to have substantial impact on the result of the present analysis. It is conservatively assumed that the systematic error is at most 25 per cent of the statistical error of $\Delta\mu/\mu$ derived in the present analysis.

5 RESULT

Based on the results provided in Table 2,

$$\Delta\mu/\mu = (-0.68 \pm 2.70_{\rm stat} \pm 0.66_{\rm sys}) \times 10^{-5}$$

is adopted as the fiducial result for the analysis of molecular hydrogen absorption in the Q2348−011 spectrum [or $\Delta\mu/\mu = (-0.68 \pm 2.78) \times 10^{-5}$, adding the uncertainties in quadrature]. The result is consistent with no change in μ at the 10^{-5} level.

The analysis of H_2 absorption in the Q2348−011 spectrum yields a result on $\Delta\mu/\mu$ which is less tight compared to the constraints from previous analyses (Ubachs et al. 2011). One of the major causes that led to the larger uncertainty is the relatively low S/N ratio of the spectrum. The second cause is that the number of lines is relatively small: 32 compared to e.g. 90 in the sightline of J2123−0050, which yields an order of magnitude more precise result on $\Delta\mu/\mu$ (Malec et al. 2010; van Weerdenburg et al. 2011). Part of the H_2 spectrum in Q2348−011 is obscured by the neutral hydrogen features of the additional strong DLA at $z \simeq 2.615$ making some of the relevant transitions unavailable. The H_2 transitions falling at the short wavelength range of the spectrum are especially useful in μ-variation analysis, since they exhibit the larger sensitivity coefficients. In the spectrum of Q2348−011, they are not detected due to the H I absorption produced by the additional DLA and another strong absorber at $z \simeq 2.93$. However, the present analysis demonstrates that a complex absorption structure can be successfully modelled by means of the comprehensive fitting method.

6 CONCLUSION

Molecular hydrogen features present at redshift $z_{\rm abs} \simeq 2.426$ in the line of sight to the quasar Q2348−011 were analysed to detect a possible variation of the proton-to-electron mass ratio on a cosmological time-scale. The constraint derived in the analysis is $\Delta\mu/\mu = (-0.68 \pm 2.78) \times 10^{-5}$, showing no indication that μ in this particular absorber is different from μ measured in the laboratory. Although being less accurate than other recent H_2 constraints on $\Delta\mu/\mu$, the result is consistent with those results, which show that $|\Delta\mu/\mu| < 1 \times 10^{-5}$ at $z = 2$–3.

In the sample of known high-redshift H_2 absorbers, the structure of the absorber in the Q2348−011 spectrum is the most complex as it has seven visually distinguishable velocity components, whilst 12 are justified statistically. The present analysis shows the applicability of the comprehensive fitting method in a case of such a complex structure. However, it also shows that in order to achieve a competitive result on $\Delta\mu/\mu$, the H_2 absorber/spectrum selected for analysis must obey several conditions among which are no occurrence of strong additional absorbers and a sufficiently high S/N.

ACKNOWLEDGMENTS

This work is based on observations carried out at the European Southern Observatory (ESO) under programme ID 79.A-0404(A) (PI Ubachs), with the UVES spectrograph installed at the Kueyen UT2 on Cerro Paranal, Chile. Additional data from the ESO-archive were used from programme ID 072.A-0346(A). JB would like to acknowledge F. van Weerdenburg and A. Malec, for assistance with using VPFIT and fruitful discussions. MTM thanks the Australian Research Council for a QEII Research Fellowship (DP0877998). WU acknowledges support from the Netherlands Foundation for Fundamental Research of Matter (FOM).

REFERENCES

Bailly D., Salumbides E. J., Vervloet M., Ubachs W., 2010, Mol. Phys., 108, 827

Ivanov T. I., Roudjane M., Vieitez M. O., de Lange C. A., Tchang-Brillet W.-Ü. L., Ubachs W., 2008, Phys. Rev. Lett., 100, 093007

Ivanov T. I., Dickenson G. D., Roudjane M., Oliveira N. De, Joyeux D., Nahon L., Tchang-Brillet W.-Ü. L., Ubachs W., 2010, Mol. Phys., 108, 771
King J. A., Webb J. K., Murphy M. T., Carswell R. F., 2008, Phys. Rev. Lett., 101, 251304
King J. A., Murphy M. T., Ubachs W., Webb J. K., 2011, MNRAS, 417, 3010
Ledoux C., Petitjean P., Srianand R., 2003, MNRAS, 346, 209
Ledoux C., Petitjean P., Fynbo J. P. U., Moller P., Srianand R., 2006, A&A, 457, 71
Malec A. L. et al., 2010, MNRAS, 403, 1541
Meshkov V. V., Stolyarov A. V., Ivanchik A., Varshalovich D. A., 2006, J. Exp. Theor. Phys. Lett., 83, 303
Murphy M. T., Tzanavaris P., Webb J. K., Lovis C., 2007, MNRAS, 378, 221
Murphy M. T., Webb J. K., Flambaum V. V., 2008, MNRAS, 384, 1053
Noterdaeme P., Petitjean P., Srianand R., Ledoux C., 2007, A&A, 469, 425
Petitjean P., Ledoux C., Noterdaeme P., Srianand R., 2006, A&A, 456, L9
Philip J., Sprengers J. P., Cacciani P., de Lange C. A., Ubachs W., 2004, Applied Phys. B: Lasers and Optics, 78, 737
Reinhold E., Buning R., Hollenstein U., Ivanchik A., Petitjean P., Ubachs W., 2006, Phys. Rev. Lett., 96, 151101
Salumbides E. J., Bailly D., Khramov A., Wolf A. L., Eikema K. S. E., Vervloet M., Ubachs W., 2008, Phys. Rev. Lett., 101, 223001
Srianand R., Petitjean P., Ledoux C., Ferland G., Shaw G., 2005, MNRAS, 362, 549
Thompson R., 1975, Astrophys. Lett., 16, 3
Thompson R. I. et al., 2009, ApJ, 703, 1648
Ubachs W., Buning R., Eikema K. S. E., Reinhold E., 2007, J. Mol. Spectrosc., 241, 155
Ubachs W., Bagdonaite J., Murphy M. T., Buning R., Kaper L., 2011, in Martins C., Molaro P., eds, Astrophys. Space Science Proc., From Varying Couplings to Fundamental Physics. Springer, Berlin, p. 125
van Weerdenburg F., Murphy M. T., Malec A. L., Kaper L., Ubachs W., 2011, Phys. Rev. Lett., 106, 180802
Varshalovich D. A., Levshakov S. A., 1993, Soviet J. Exp. Theor. Phys. Lett., 58, 237
Wendt M., Molaro P., 2010, A&A, 526, A96
Wendt M., Reimers D., 2008, Eur. J. Phys. D Special Topic, 163, 197
Whitmore J. B., Murphy M. T., Griest K., 2010, ApJ., 723, 89

This paper has been typeset from a TEX/LATEX file prepared by the author.